International Journal of Electric Power and Energy Studies
ISSN: 3006-2004 (Print), ISSN: 3006-0826 (Online) | Volume 5, Number 2, Year 2026
DOI: https://doi.org/10.62051/ijepes.v5n2.02
Journal homepage: https://wepub.org/index.php/IJEPES/index

Optimization the Light-Heat-Biomass Synergistic Hydrogen Production System in High-Altitude

Xiaoqing Yang*, Shuang Bai

School of Economics and Management, Southwest Petroleum University, Chengdu, Sichuan, 610500, China

*E-mail: y2813459894@163.com

ABSTRACT

In high-altitude areas, resources are abundant and energy consumption is decentralized, and the energy system has not achieved interconnection. Hydrogen energy, as a clean energy source, can fully utilize the resources in high-altitude areas and achieve large-scale utilization of energy and chemicals, cross-time and regional transportation, and integration of various energy sources. Based on this, this paper constructs a multi-energy complementary system including electricity, heat, oxygen, and hydrogen, focusing on multi-path collaborative improvement of hydrogen and oxygen production, full utilization of photothermal resources, and enhancing system economic efficiency. It proposes an innovative operation framework for a photothermal-biomass combined hydrogen production plant. By integrating CO_2 electrolysis oxygen circulation technology and photovoltaic green hydrogen auxiliary mechanism, a photothermal-biomass collaborative hydrogen production system is constructed. Firstly, a system mathematical model is built and chemical simulation analysis is conducted to verify the feasibility of the hydrogen production route. Secondly, the energy/energy efficiency of the hydrogen production system is analyzed from the perspectives of hydrogen/oxygen production rate and energy/energy efficiency. Finally, economic analysis is conducted to calculate the levelized hydrogen production cost to verify economic feasibility.

KEYWORDS

Light-Thermal-biomass Co-production of Hydrogen; Biomass Gasification; Aspen Plus Simulation; Flat-rate Hydrogen Production Cost.

1. ITRUDUCTION

Hydrogen energy, as a clean secondary energy source, has been vigorously promoted and developed under the background of the “dual carbon” goals [1]. Due to its characteristics of low volumetric energy density, high gravimetric energy density, and low carbon emissions, extensive research has been conducted across all stages of production, storage, transportation, and utilization [2]. At present, hydrogen production still mainly relies on fossil fuels, which not only leads to significant carbon emissions but also restricts the sustainable development of the hydrogen energy industry. Based on this, a large number of studies have explored renewable hydrogen production pathways, with the main technologies including biomass pyrolysis/gasification and renewable-driven water electrolysis [3][4].

Previous studies include hydrogen production using coalbed methane, which is inexpensive and easily accessible[5]. Methane enrichment is achieved through low-energy-consumption purification processes such as pressure swing adsorption and temperature swing adsorption, thereby enabling low-cost and low-carbon-emission hydrogen production. Hydrogen production via natural gas reforming involves the reaction of methane with steam under high temperature and catalytic conditions to

produce hydrogen, which features low carbon emissions but relatively high costs[6]. Regarding photocatalytic water splitting for hydrogen production, studies have investigated carbon nitride and cadmium sulfide nanomaterials with suitable band structures as photocatalysts, which not only facilitate the separation and migration of photogenerated charge carriers but also ensure strong redox capability[7]. In terms of solar thermochemical hydrogen production[8][9], the NEOM green hydrogen project in Saudi Arabia utilizes large-scale solar thermal systems to produce green hydrogen, achieving off-grid energy self-sufficiency and ensuring reliable energy supply. For seawater hydrogen production[10], various hybrid seawater electrolysis schemes have been proposed by coupling small-molecule substitution anodic oxidation reactions with cathodic hydrogen evolution reactions, enabling safe and efficient seawater splitting and environmental pollutant treatment. In the field of biomass hydrogen production[11], the concept of "ultra-green hydrogen" has been proposed, establishing a hydrogen production pathway based on lignocellulosic biomass such as straw, integrating "waste utilization–energy conversion–carbon reduction," thereby further enriching sustainable hydrogen production systems.

With the development of renewable energy, the coupling of green electricity and hydrogen has become a research hotspot[12][13]. Under scenarios of limited grid accommodation capacity, surplus renewable energy can be locally consumed to drive electrolyzers for water splitting and hydrogen production, becoming one of the important approaches for green hydrogen production. Regarding alkaline water electrolysis[14], it has been developed for many years abroad and is a mainstream hydrogen production technology, featuring good stability and cost-effectiveness; however, it is relatively weak in equipment manufacturing. Domestic research mainly focuses on reducing power consumption, increasing hydrogen production, improving response speed, and extending service life. As for proton exchange membrane (PEM) water electrolysis[15], it has been widely studied due to its low resistance, high current density, high hydrogen purity, and fast response speed. The core lies in breakthroughs in catalyst activity and stability, including platinum nanocluster catalysts, iridium oxide catalysts, and ruthenium oxide catalysts.[16][17]

This paper proposes to carry out research in high-altitude regions based on local conditions, considering the abundance of photovoltaic and biomass resources, to achieve reliable energy supply and stable operation of integrated electricity–heat–oxygen–hydrogen systems[18][19]. However, overall research on large-scale hydrogen production and utilization oriented toward the special geographical environment of high-altitude regions remains relatively limited.

2. MULTI-PATH COLLABORATIVE HYDROGEN PRODUCTION SYSTEM MODEL

2.1. Photovoltaic Hydrogen Production

Regarding hydrogen production through photovoltaic-electrolyzer, the terrain and natural environment in high-altitude areas are complex and variable. This paper constructs a dual-array structure photovoltaic-electrolyzer system, using two independent photovoltaic systems and electrolyzer systems. It mainly consists of photovoltaic arrays and electrolyzer arrays, which are composed of several photovoltaic modules and electrolyzer units connected in series and parallel. Among them, the intensity of light and temperature have a significant impact on the photovoltaic power generation system, and their output I-U curve is nonlinear. The photovoltaic modules convert solar energy into electricity and supply it to the electrolyzer for water electrolysis to produce hydrogen. Due to environmental limitations, this paper studies the direct coupling situation of photovoltaic and electrolyzer, but direct coupling requires a high matching capability, and at the same time, the natural environment changes in real time, leading to a mismatch situation, which further results in energy loss.

The proton exchange membrane electrolyzer has the characteristics of rapid start-up and shutdown, fast response, and low current density, making it suitable for intermittent and fluctuating photovoltaic power generation systems. Meanwhile, hydrogen transportation through pipelines requires pressurized hydrogen, and PEM with higher pressure has the advantage of matching the hydrogen storage requirements. Therefore, this article selects the proton exchange membrane electrolyzer, with ions and electrons flowing through water and physical equipment respectively[20].

2.2. Photothermal-Biomass Hydrogen Production

The photovoltaic resources are abundant in high-altitude areas. During the day, we can utilize the abundant solar energy and convert it into thermal energy to provide industrial steam for the drying and cracking of biomass. This can fully utilize the sunlight and reduce the cost of steam. At the same time, waste resources such as straw, sawdust, leftover food, and fruit shells can be transformed from "waste" to "treasure". Therefore, this paper selects the thermochemical hydrogen production technology. Firstly, the trough-type concentrating panels are used to concentrate solar radiation onto the heat-absorbing tubes, raising the temperature of the high-temperature oil to around 390℃ and storing it in the molten salt tank to provide continuous heat for the subsequent steps. The stored hot oil preheats water to become industrial steam, which is sent into the downward-flowing fixed-bed gasifier as a gasification agent to provide gasification for biomass. Research shows[21] that pure steam as a gasification agent can significantly increase the hydrogen production and maintain a certain economic efficiency.

In high-altitude areas, there is a large amount of stored wood-based straw such as cotton straw, and it has great potential for hydrogen production. This paper selects cotton straw as the raw material[22]. The composition analysis is as follows:

Table 1. Components

Biomass	Industrial analysis/%				Elemental analysis/%					Low calorific value/(MJ/kg)
	V_{dr}	FC_{ar}	M_{ar}	A_{ar}	C	H	O	N	S	
Cotton stalks	72.45	14.12	6.16	7.27	48.34	5.7	45.83	0.13	0	15.37

3. EQUIPMENT SELECTION AND CONFIGURATION FOR THE SYNERGISTIC HYDROGEN PRODUCTION SYSTEM

3.1. Mathematical Modeling of Subsystems

Due to the uncertainties such as the intermittent nature of solar energy resources and the efficiency decline of equipment in low-temperature environments in the multi-path collaborative hydrogen production system in high-altitude areas, as well as the involvement of multi-device coupling and multi-energy flow operation in this process, the reliable operation of the system and the continuous production of hydrogen face significant challenges. Therefore, this paper establishes a hierarchical collaborative optimization method: the photothermal-biomass hydrogen production subsystem uses Aspen Plus for the entire process thermodynamic simulation to determine the key equipment parameters and operating conditions; the photovoltaic-electrolyzer subsystem simulates the electrolyzer's water electrolysis characteristics through the Aspen Custom Modeler sub-program, and then imports it into the Aspen Plus software to simulate the hydrogen production process, outputting the U-I curve. Each system meets the voltage, energy, and material constraints to meet the automatic switching of operation modes under special scenarios. To further verify the technical feasibility of this paper, this paper conducts analysis from the aspects of mass conservation and energy efficiency:

first, through the entire process material balance to verify the mass balance of the system; second, combined with thermodynamic analysis and Faraday efficiency calculation to evaluate the energy conversion efficiency, ensuring the reliability of the theoretical model and engineering practice.

3.1.1. Photovoltaic - Alkaline Electrolyzer for Water Electrolysis to Produce Hydrogen

The article further explores the power generation characteristics of photovoltaic modules based on their specific properties[23], and matches the power consumption characteristics of the electrolytic cell to achieve the optimal utilization of resources in the series-parallel structure.The voltage of a single electrolytic cell is:

$$U_{el} = U_{rev} + U_{ohm} + U_{act} + U_{diff} \tag{1}$$

The calculation formulas for each of these variables are as follows:

$$U_{rev} = U_{rev}^{0} + \frac{RT}{2F}\ln\left(\frac{P_{H_2}\sqrt{P_{O_2}}}{a_{H_2O}}\right) \tag{2}$$

$$U_{act} = \frac{RT}{\alpha\, n\, F}\ln\left(\frac{i_{el}}{i_0}\right) \tag{3}$$

$$U_{ohm} = i \cdot A \cdot R_{ohm} \tag{4}$$

The electrolytic cell, when matched with the photovoltaic system, needs to take into account the current and voltage determined by its series-parallel structure. Its mathematical model is:

$$\begin{cases} U_{stack} = n_s U_{el} \\ I_{stack} = n_p I_{el} \end{cases} \tag{5}$$

The formula for the Faraday efficiency is as follows:

$$\eta_f = 100\exp\left(\frac{(-b_1[1-(P-1)b_2])}{i_{el}}\right) \tag{6}$$

The formula for hydrogen production efficiency is:

$$r_{H_2} = \frac{\eta_F I_{stack}}{2F} \tag{7}$$

3.1.2. Photothermal-Biomass Gasification for Hydrogen Production

Thermal-hydrogen production from biomass mainly involves using trough-type solar collectors to provide heat for the gasification process of biomass to produce hydrogen. At the same time, the design includes a water-gas shift reaction to convert the CO products from the gasification process into water gas, generating a large amount of CO_2 which can be collected and sealed for carbon capture

technology, and used for CO_2 electrolysis to further increase hydrogen production. Aportion of the produced O_2 is used in the combustion process to reduce the heating cost.

Parabolic trough-type concentrating solar collectors[24] components mainly consist of steel supports, tracking devices, concentrating mirrors, and heat absorption tubes. The equipment gathers sunlight into the heat absorption tubes, causing the heat transfer oil inside the tubes to heat up, achieving the conversion of solar energy to thermal energy. The concentrated solar energy received by the heat absorption tubes is:

$$Q_{solar} = I \cdot \cos\theta \cdot \kappa_{IAM} \cdot \eta_{opt} \cdot L_{PTC} \cdot W_{PTC} \tag{8}$$

the formula is as follows:

$$Q_{heatloss} = [\alpha_1(T_{PTC} - T_{atm}) + \alpha_4(T_{PTC} - T_{atm})^4]L_{PTC} \tag{9}$$

The actual collected effective solar energy :

$$E_{solar} = Q_{solar} - Q_{heatloss} = \dot{m}_{\mathrm{HTF}}(h_{out} - h_{in}) + M \cdot h_{\mathrm{HTF}} \tag{10}$$

Through the trough-type concentrating - molten salt dual-tank energy storage for heat storage, the oil-salt heat exchanger passes through the steam generation system, generating superheated steam at 370 - 420℃ and 1.5 - 3MPa, and directly discharging the steam into the downward-inlet fixed-bed gasifier. In the gasifier, the specific process is as shown in Figure 1:

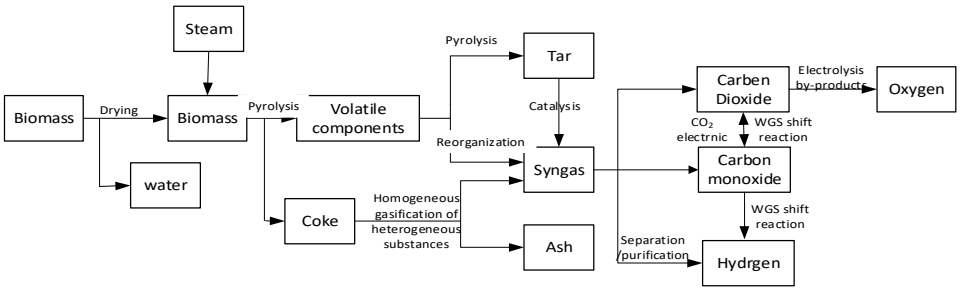

Figure 1. Biomass Steam Gasification Process

The biomass materials such as straw and sawdust contain moisture by themselves. They are first naturally air-dried and then ground and sieved to increase their specific surface area. Then, they are sent to the gasification furnace to be heated and the excess moisture evaporated, reducing their moisture content to below 5%. The dried biomass undergoes pyrolysis and reacts with steam to produce syngas. The pressure is 30 MPa and the temperature is 900°C. The oxygen-rich zone and some carbon in the furnace self-burn to provide heat, while the molten salt water vapor serves as the gasification agent and temperature regulation means. Above 850°C, the high temperature and reduction of steam decrease the generation of tar during the cracking process. Besides, the main factors affecting hydrogen production are the characteristics of the biomass materials, the amount of steam injection, and the particle size of the materials. Based on the existing properties of biomass in high-altitude areas, we try to select materials with lower moisture content and smaller particle size to

increase the heat transfer rate. Steam participates in reactions such as carbon gasification, water gas shift, and compound reforming. Generally, with the increase in steam volume, the reaction proceeds further. However, unrestricted increase will lead to an increase in cost. Therefore, this paper designs the S/B ratio of steam/biomass as 2[25] to ensure economic efficiency while increasing the carbon conversion rate and gas production rate.

The overall chemical reaction equation in the gasifier:

$$CH_xO_yN_z + H_2O(l) + O_2 \rightarrow H_2 + CO + CO_2 + H_2O(g) + CH_4 \tag{11}$$

To facilitate the reaction process, the gasifier operation requires energy consumption, which is directly proportional to the processing volume and calorific value of the raw materials and is significantly influenced by the operating temperature. There exists an optimal temperature range for electricity consumption. Meanwhile, the greater the electricity power consumed by the gasifier, usually means that it generates more residual heat. Through a heat recovery system (such as a waste heat boiler), a portion of the residual heat can be captured and used for heating or to drive other equipment, thereby improving the overall energy utilization efficiency. The specific energy consumption calculation formula is as follows:

$$q_{i,t}^{gasf} = \frac{k_1 \, \eta^{gasf} \, m_{i,t}^{gasf} \, O^{gasf}}{2C^{H_2}} \tag{12}$$

$$h_{i,t}^{rec} = \eta^{rec} \, P_{i,t}^{gasf} \tag{13}$$

$$P_{i,t}^{gasf} = \frac{\eta^{gasf} \, m_{i,t}^{gasf} \, H^{gasf}}{1+\left(\frac{T_{i,t}^{gasf}}{T^{ref}}\right)^{\mu}} \tag{14}$$

(1) Water-gas Shift Reaction

This paper selects CeO_2 as a transition metal catalyst, which enhances performance through the synergistic effect of the carrier's interface. It is not only inexpensive but has also completed large-scale commercial applications. In the water-gas shift reaction, H_2O adsorbed on the catalyst surface decomposes into OH and H, while the adsorbed CO reacts with OH to form carbon oxide compounds such as formate, and these intermediates further decompose to form CO_2 and H_2 and other products, which are desorbed on the catalyst surface.

The water-gas shift reaction is an exothermic and entropy-increasing process. To promote the reaction, not only high-temperature steam is required, but also a circulation pump is needed to increase the gas flow rate on the catalyst surface and a temperature control device is needed to maintain the optimal reaction temperature. During this chemical reaction process, the hydrogen production rate and the heat/electric power requirements are as follows:

$$q_{i,t}^{H_2} = \eta_{i,t}^{WGS} \cdot F_{i,t}^{CO,in} \cdot X_{CO} \tag{15}$$

$$P_{i,t}^{WGS,heat} = \frac{F_{i,t}^{CO,in} \cdot \Delta H_{rxn}^{WGS}}{\eta_{heat}} \quad (16)$$

$$P_{i,t}^{WGS,elec} = P_{i,t}^{WGS,heat} + P_{i,t}^{pump} + P_{i,t}^{control} \quad (17)$$

(2) Carbon Capture and CO_2 Electrolysis

After the synthesis gas from the water-gas shift reaction undergoes hydrogen purification and desulfurization and denitrification, it is sent from the bottom into the absorption tower of the carbon capture system. At the same time, it collides with the MEA (monoethanolamine) aqueous solution injected from the top of the tower, absorbs carbon dioxide, and then flows out from the bottom, becoming MEA-rich liquid. It first passes through the heat exchanger between the rich and poor liquid to obtain heat, then is heated and enters the desorption tower. At a temperature of 200℃, CO_2 automatically escapes from the top and is desorbed, and is then dried and dehydrated before being sent to the CO_2 electrolysis device. The remaining gases are mainly hydrocarbons, which are sent to the gasifier for combustion and heating. Meanwhile, the rich liquid becomes poor liquid and re-enters the cycle of capturing CO_2 [26].

The specific calculation formula is as follows.

$$W_{CO_2ER} = \left(\frac{\dot{n}_{CO_2,in} \cdot X_{CO_2} \cdot z \cdot F}{\eta_{Faradaic}}\right) \cdot V_{Cell} \quad (18)$$

$$CO_{generation} = \dot{n}_{CO_2,in} \cdot X_{CO_2} \quad (19)$$

$$O_{2_{generation}} = 0.5 \cdot \dot{n}_{CO_2,in} \cdot X_{CO_2} \quad (20)$$

3.2. System Thermodynamic Analysis

Regarding the hydrogen production system using electrolyzers, the existing simulation studies based on Simulink mostly focus on individual systems and lack comprehensive research on the entire hydrogen production process. Therefore, this paper introduces the Aspen Custom modeler (a subroutine of Aspen Plus) to establish a PEM electrolyzer model and simulate the hydrogen production process of multiple PEM electrolyzers. Based on this, the modeling of the hydrogen production process of the photothermal-electrolyzer system is carried out and integrated into Aspen Plus for thermodynamic analysis. Regarding the modeling and simulation analysis of the photovoltaic hydrogen production system, the main goal is to achieve voltage, material, and energy balance. The specific formulas are as follows:

Total voltage equation:

$$V_{cell}(T, p, I) = V_{id} + \Delta V_{act} + \Delta V_{ohm} \quad (21)$$

Ideal voltage:

$$V_{id} = \frac{\Delta G^{\circ}(T, p_{ref})}{nF} + \frac{RT}{nF} \ln\left(\frac{p_{H_2} p_{O_2}}{a_{H_2O}}\right) \tag{22}$$

Activation overvoltage:

$$\Delta V_{act} = \frac{RT}{nF\alpha_X} \ln\left(\frac{i_X}{i_{0,X}}\right) \tag{23}$$

Ohmic polarization voltage:

$$\Delta V_{ohm} = iR_{ohm} \tag{24}$$

The calculation formula for the production of oxygen and hydrogen:

$$F_{H_2} = A_{cell} \frac{ni}{2F} \eta \tag{25}$$

$$F_{O_2} = A_{cell} \frac{ni}{4F} \eta \tag{26}$$

Regarding the molar mass of water, in the electrolytic cell, water mainly flows between the positive and negative electrodes through electroosmosis and diffusion flow. The formula for calculating the molar mass flow rate of the final reaction is as follows:

$$F_{H_2O}^{eo} = n_d \frac{i}{F} M_{H_2O} A_{cell} n \tag{27}$$

$$F_{H_2O}^{diff} = D_w \frac{c_{wa} - c_{wc}}{t_m} M_{H_2O} A_{cell} n \tag{28}$$

Energy balance:

$$H_{out} = P_{el} + H_{in} - Q_{loss} \tag{29}$$

Regarding the photothermal-biomass hydrogen production system, this paper uses Aspen Plus to simulate the production process and reveals the conversion laws of energy and work within the system, as well as the energy losses. To simulate the technical feasibility of this process in high-altitude areas, the efficiency of the system is reflected by the following several indicators, and its feasibility is verified by comparing with the experimental results.

1) Energy required for the reaction process

The total heat energy required to maintain the system's reaction is composed of the heat loads of the heat exchanger, the yield reactor, and the Gibbs reactor. Taking into account the heat loss during the heat transfer process, the calculation formula for the energy that the solar energy system needs to provide is:

$$Q_{solar} = \frac{Q_{HX_2} + Q_{RYIELD} + Q_{RGIBBS}}{0.9} \tag{30}$$

2) Refrigerant gas efficiency

The refrigerant gas efficiency is used to evaluate the direct conversion efficiency of the gasification process in converting the chemical energy input from the biomass into the chemical energy of the product syngas.

$$\eta_c = \frac{\sum m_i H_{L-i}}{m_{biomass,daf} H_{L-biomass,daf}} \times 100\% \tag{31}$$

$$\sum m_i H_{L-i} = m_{CO} H_{L-CO} - m_{CH_4} H_{L-CH_4} + m_{H_2} H_{L-H_2} \tag{32}$$

3) Energy Efficiency

Overall evaluation of the total energy utilization efficiency of the entire system from a quantitative perspective, taking into account all energy inputs and outputs.

$$\eta_{en} = \frac{E_{out}}{E_{in}} \times 100\% \tag{33}$$

$$E_{in} = E_{WS} + E_{solar} + E_{pump} \tag{34}$$

$$E_{out} = E_{syngas} + E_{ele} \tag{35}$$

4) Exergy Efficiency

Comprehensively evaluate the effective energy utilization efficiency of the entire system from the perspective of quality. Exergy is the maximum portion that can be converted into useful work theoretically, and exergy efficiency reflects the degree of system perfection.

$$\eta_{ex} = \frac{E_{x,out}}{E_{x,in}} \times 100\% \tag{36}$$

$$E_{x,in} = E_{x,WS} + E_{x,solar} + E_{x,pump} \tag{37}$$

$$E_{x,out} = E_{x,CO} + E_{x,CH_4} + E_{x,H_2} + E_{x,ele} \tag{38}$$

3.3. Process Simulation

The energy technology evaluation of the co-production hydrogen system is mainly based on the hydrogen production efficiency of the system, the efficiency of the cold gas, and the power consumption required. Considering the special geographical environment of high-altitude areas, the system process is established in Aspen Plus, with a fixed pressure, and five operating conditions are set by combining different reaction temperatures (600, 650, 700, 750, 800, 900°C) and biomass input energy (215.14 ~ 1075.70 kW). For each operating condition, the simulation results of the software are used as input and substituted into the above formulas to calculate the syngas yield, cold gas efficiency, energy efficiency, exergy efficiency, and system net work, thereby determining the optimal operating condition of the system.

When using the software material analyzer to conduct material analysis for the reactants, a process simulation is carried out again. For each step of the reaction simulation, first, understand the reaction process based on the aforementioned information, input the basic information of the reactants. Then, using the Peng-Robinson with Boston Matnos material reactor, including reaction temperature and pressure, finally, based on the Aspen pius model which is constructed using the Gibbs minimum free energy method, set the temperature, pressure and gasifying agent, and simulate the final product content.

3.4. Discussion of Results

3.4.1. Model Validation

The comparison of the simulation results with the actual results is shown in Table 2 below. According to the relative error results, it can be seen that there are small differences in the current, voltage and operation conditions of the model, but the relative error of hydrogen production rate is small, and the energy consumption is basically the same, indicating that the electrolyzer hydrogen production process can be accurately simulated.

Table 2. Parameter Verification Comparison

Parameters	Simulated data	Actual date	Relative error
Voltage/V	196.5	203	3.3%
Electric current/A	498.3	506.5	1.6%
Real-time power/kW	97.4	102.8	5.5%
Hydrogen production rate/(m^3/h)	23.4	22.8	2.5%
Pre-slag temperature/°C	48	45	6.2%
Back-end temperature/°C	58	55	5.2%
Anode pressure/MPa	2.8	2.8	0
Cathode pressure/MPa	3.0	3.0	0
Energy consumption/(KWh/m^3)	4.5	4.509	0.2%

To verify the simulation process of the photothermal-biomass hydrogen production system, this paper compares the simulation results with those from other articles and calculates the average relative error between the simulation and the actual results to verify the accuracy of the model. Among them, the CO recovery and CO_2 capture and electrolysis part differs from those in other papers, so it is not included in the overall simulation process.

3.4.2. Comparison of Hydrogen/Oxygen Production Rates

The light intensity is shown in the following figure. During the process of generating electricity with photovoltaic panels, the power generation capacity is directly related to the solar radiation. Therefore, the current density changes with the variation of light intensity, as shown in Figures 2 and 3. The current density is proportional to the light intensity, and reaches its peak at noon. The simulation results of hydrogen/oxygen production are shown in Figure 4. The electrolyzer and photovoltaic panels are directly coupled through series and parallel connections. The more parallel electrolyzers there are due to stronger light, the higher the hydrogen production rate is, and it is also proportional to the current density.

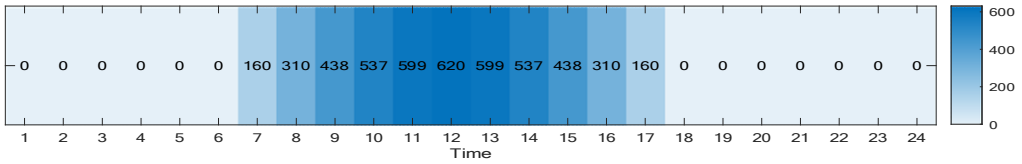

Figure 2. Typical variation of solar radiation intensity

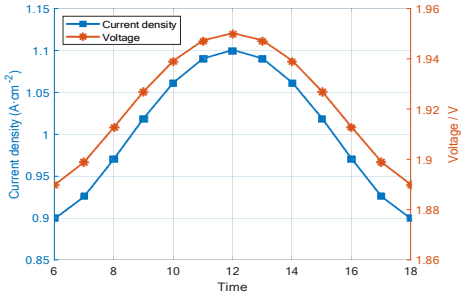

Figure 3. Changes in Current Density

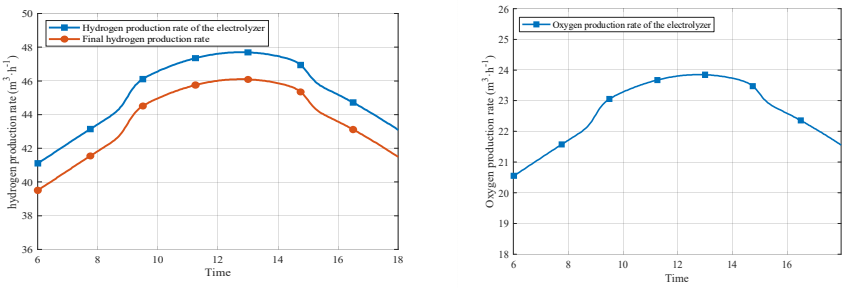

Figure 4. Comparison of hydrogen/oxygen production results

3.4.3. Thermodynamic Analysis Results

For the photothermal-biomass system, the main analysis focuses on the content of the products under different operating conditions. Since the concentration of syngas varies with the changes in reaction conditions, this paper analyzes the concentration of syngas under different operating conditions to identify the optimal operating conditions. The basic conditions of different operating conditions are shown in Table 3 The fixed reactor pressure is 25 MPa, keeping the gasifier agent in a critical state. Different temperatures are set, and the biomass concentration increases exponentially, thereby observing the concentration of syngas.

Table 3. Different operating conditions

Operating condition	Reactor pressure/MPa	Reactor temperature/°C	Biomass energy input/kW	Feed concentration/wt%
1	25	600	215.14	5
2	25	650	430.28	10
3	25	700	645.42	15
4	25	750	860.56	20
5	25	800	1075.7	25
6	25	900	1290.84	30

This paper fixed the pressure and calculated the content of syngas and the total output of the system under different temperatures and biomass concentrations. Then, it analyzed the appropriate operating conditions. Based on the simulation results, the production amounts of syngas (H_2, CO, CO_2, and CH_4) under different operating conditions are shown in the following figure. As shown in the figure, under different energy input conditions, the trends of gas production rates with temperature are generally consistent. Among them, the methane (CH_4) production rate decreases with the increase in temperature and increases with the increase in input energy; the production rates of H_2, CO, and CO_2 all increase with the increase in temperature. At higher input energy, the production rates of CH_4 and CO reach the highest, while the production rates of H_2 and CO_2 are relatively the lowest. At lower energy input, the production rate of CH_4 is more sensitive to temperature changes; with the increase in energy input, the influence of temperature on the production rate is significantly weakened. Within the range of 650-700°C, the production rate of CO shows a significant jump with the increase in temperature, but its response to energy changes is relatively insensitive

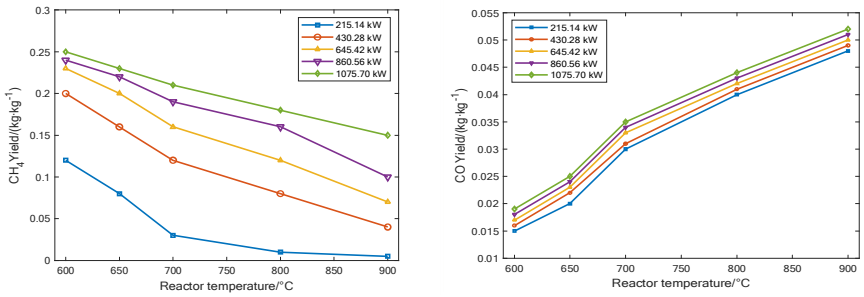

Figure 5. Changes of CH_4 /CO under Different Operating Conditions

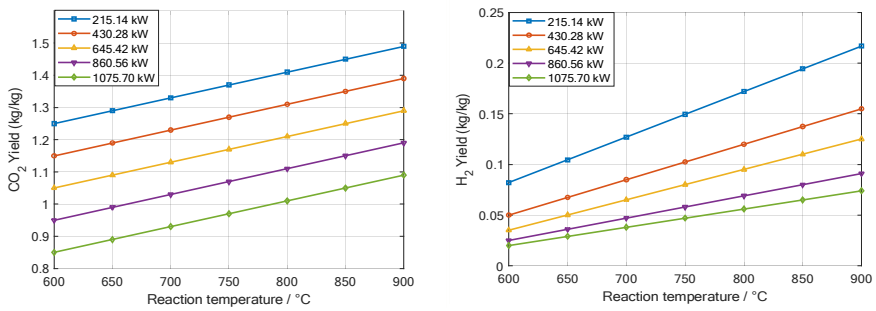

Figure 6. Changes in CO_2/H_2 under Different Operating Conditions

3.4.4. Energy and Energetic Value Analysis

The exergy efficiency and energy efficiency of the gasification system under different operating conditions are shown in Figures.when the input energy exceeds 860.56 kW and the temperature is higher than 700℃, the growth rate of efficiency slows down significantly, and further increasing the energy input or temperature has limited improvement effect on efficiency. Under the operation mode of running only during the day, the highest energy efficiency and exergy efficiency of the system are 38% and 37.6% respectively; while under the continuous operation mode throughout the day, the highest efficiencies are 36.1% and 35% respectively. Under the same conditions, the efficiency during the day operation is always about 2% to 3% higher than that during the whole-day operation.

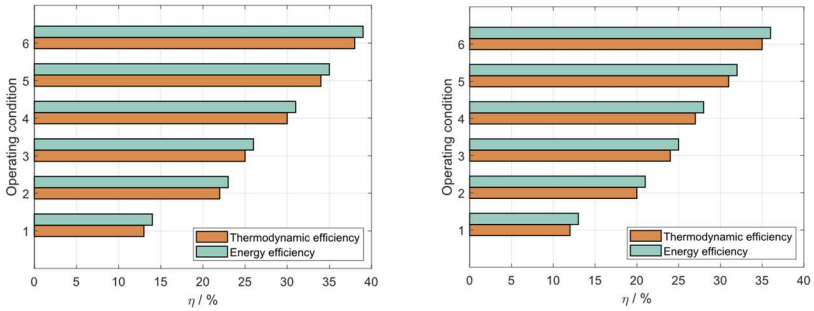

Figure 7. Energy and Exergy Efficiency during the Day/hroughout the Day

3.4.5. Sensitivity Analysis

During the process of biomass gasification for hydrogen production, different temperatures, gasifiers, and S/B ratios will have different effects on hydrogen production rate. Based on this, this paper further studies the influence of different temperatures on hydrogen production rate under different gasifier conditions, as shown in Figure 8. The hydrogen production volume is positively correlated with the reaction temperature. As the temperature increases from 600°C to 900°C, the hydrogen production gradually increases. The growth rate shows a significant change, and when the temperature is greater than 750°C, the sensitivity of hydrogen production to further increasing the temperature significantly decreases. The slopes of all trend lines become significantly smoother. A comparative analysis of different gasifiers was conducted. Under all the same temperatures, steam can produce the most hydrogen as the gasifier, followed by the air-steam mixture.

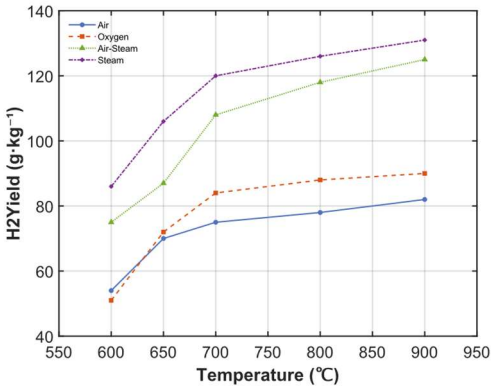

Figure 8. The influence of different gasifiers on hydrogen production rate

In the hydrogen production process using steam as the gasification agent, S/B has a significant impact on the composition of the syngas. As shown in Figure 9, the concentration of CH_4 varies little

throughout the range of S/B, and its generation path is less sensitive to this parameter; in the S/B < 1.5 range, the total yield of the syngas in the system is relatively low, and the change in S/B has a weak influence on the distribution of main components such as H_2, CO, and CO_2; when S/B > 1.5, its regulatory effect significantly enhances. Here, the yield of H_2 and CO_2 is positively correlated with S/B, and H_2 shows higher sensitivity to the increase in S/B due to the strengthening of the water-gas shift reaction.

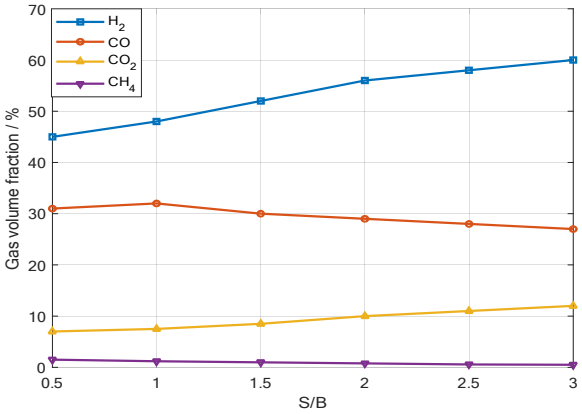

Figure 9. The influence of S/B on the components of syngas

4. CALCULATION OF SYSTEM ECONOMIC INDICATORS - ECONOMIC FEASIBILITY STUDY

This section comprehensively assesses the collaborative hydrogen production technology by calculating economic indicators, including total investment cost, annual operating cost, and levelized hydrogen production cost. These are estimated through the parameters of related equipment and economic parameters. Through the comparative analysis of economic parameters, the economic feasibility of the model proposed in this paper is verified. Finally, a sensitivity analysis is conducted to analyze the sensitivity of hydrogen production cost to changes in electricity prices, raw materials, etc., providing a reference for subsequent optimization decisions.

Table 4. Basic Parameters and Assumptions for Hydrogen Production Cost

Assumption / Parameter	Value
The lifespan of straw	2 year
Number of operating hours of the equipment	5000h
Discount rate	5%
Maintenance fee	3% Cost of Capital
Electrolytic cell current density	800mA/cm2
Industrial water usage	2 Per tonne
Grid electricity price	0.1/kwh
Renewable energy electricity price	0.085/kwh

4.1. Total Investment Cost

The total investment cost is mainly estimated through initial equipment investment, installation fees, etc. To accurately reflect the current economic situation, the model adjusts for inflation using the Chemical Engineering Plant Cost Index (CEPCI). Additionally, the replacement costs of equipment due to damage or technological updates during the project's lifespan are also taken into account. The specific calculation formula is as follows:

$$C_{\mathrm{CAPEX}} = 1.18 \cdot \sum_{j=1}^{p} \sum_{k=1}^{q} B_j \cdot C_{E,j} \cdot \frac{1}{(1+r)^{L_j(k_j-1)}} \cdot \frac{\mathrm{CEPCI}_{2025}}{\mathrm{CEPCI}_{\mathrm{Ref},j}} \tag{39}$$

4.2. Annual Operating Costs

The annual operating costs of the system consist of various consumptions and maintenance expenses during the system's operation process. They mainly include regular operating expenses, namely annual equipment maintenance costs, process water costs, oxygen costs, electricity input costs, which are further divided into grid electricity cost and renewable energy electricity cost. Since this process uses solar radiation and wheat straw as raw materials, this model assumes that these costs are zero. The specific calculation formula is as follows:

$$C_{\mathrm{OPEX}} = C_M + C_W + C_{GE} + C_{RE} \tag{40}$$

Among them, C_M represents the annual raw material cost, C_W represents the annual water cost, which includes process water, cooling water, boiler feed water, etc., C_{GE} represents the annual purchased electricity/energy cost, and C_{RE} represents the annual other miscellaneous and labor costs, including maintenance fees, labor costs, insurance, taxes, etc.

4.3. Standardized Hydrogen and Oxygen Production Costs

The standardized cost is the core indicator for evaluating this technical model. It mainly considers the hydrogen production volume and allocates capitalized expenditures and operating costs to each year. The higher the production volume, the more obvious the economic advantage of this technology. The specific calculation formula is as follows:

$$\mathrm{LCOH} = \frac{C_{\mathrm{CAPEX}} \cdot \mathrm{CRF} + C_{\mathrm{OPEX}}}{m_{\mathrm{H_2}} \cdot 8{,}000} \tag{41}$$

$$\mathrm{CRF} = \frac{r \cdot (1+r)^{\mathrm{PL}}}{(1+r)^{\mathrm{PL}} - 1} \tag{42}$$

4.4. Discussion of Results

The calculation of capital expenditures and operating expenditures is shown in Table 7. This paper conducts a comprehensive economic comparison analysis between the proposed integrated process of electrolyzing water to produce hydrogen and gasifying biomass and the benchmark biomass gasification process. The integrated process has increased both capital expenditures and operating expenditures. The main reason for this is the introduction of key equipment such as electrolyzers and CO_2 recovery and purification systems, which led to an increase in CapEx by approximately 35%. At the same time, this process consumes a large amount of industrial water and renewable energy

electricity, resulting in an increase in OpEx by approximately 19%. However, thanks to the synergistic effect of the electrolyzing water and CO_2 electrolysis units, the integrated process significantly reduces CO_2 emissions while achieving a substantial increase in hydrogen production.

By calculating the total investment and operating costs, we can gain a detailed understanding of the main expenses of the process described in this article. To further verify the economic viability of the technology presented in this article, we calculate its normalized hydrogen production cost and compare it with the basic process, as shown in the following figure. The normalized hydrogen production cost has decreased by 1.1%, and the cost of the overlapping part of the process is basically the same. Even if the electrolyzer and CO_2 capture- electrolysis equipment are added, since the water electrolysis mainly utilizes renewable energy sources such as photovoltaics, and the recovered CO_2 electrolysis increases the hydrogen production volume, the hydrogen production cost is averaged out, resulting in a decrease in the normalized cost, proving the economic feasibility of the technology.

Table 5. The cost comparsion

Cost estimation	Gasification (ten thousand yuan)	Electrolysis of water - Gasification - CO2 electrolysis (ten thousand yuan)
Capital expenditure		
Electrolytic cell	—	300
Compressor	404.5	439.4
Turbine	29.28	30.32
Pump	25.17	25.4
Heat exchanger	93.73	85.5
Refrigerator	650	650
WGS Reactor	210.9	240.2
PSA Separator	3.8	8.2
CO2 Recycling	—	136.32
Total capital expenditure	1417.38	1915.34
Operating expenses		
Maintenance fee	45.3	67.4
Process water cost	35.7	96.3
Oxygen	43.72	—
Electricity of the power grid	68.2	36.7
Renewable energy electricity	—	90.6
Total operating expenses	242.93	291

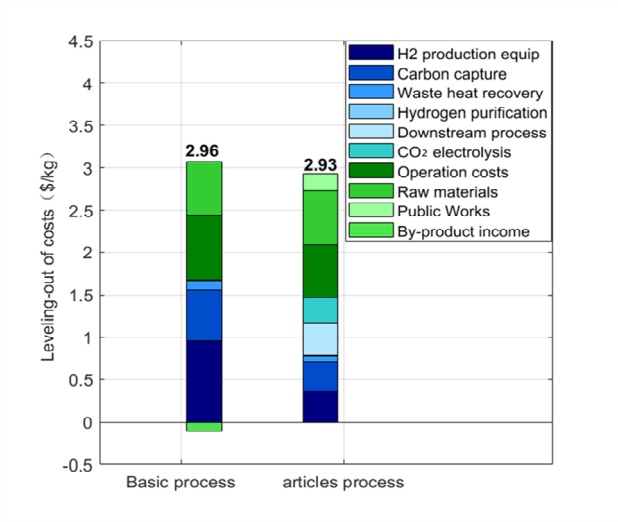

Figure 10. Comparison of Standardized Hydrogen Production Costs

The hydrogen production process proposed in this paper has a significant cost advantage compared to the basic biomass gasification hydrogen production method. In the context of the rapid development of current hydrogen production technologies, various routes such as electrolysis water hydrogen production (including alkaline electrolyzers and coupling with renewable energy), methane reforming hydrogen production, and food waste gasification hydrogen production have become relatively mature. The comparison analysis is as shown in Table 6. Hydrogen production technology coupled with carbon capture can achieve green hydrogen production, and the energy efficiency is generally maintained above 65%. Among them, the path of alkaline electrolyzer coupled with renewable energy shows a higher energy efficiency and lower standardized hydrogen production cost. Methane steam reforming hydrogen production has a lower cost but lower energy efficiency. While food waste gasification hydrogen production has a higher cost.

Table 6. Comparison of Costs of Different Technologies

Hydrogen production process route	Hydrogen type	Energy efficiency(%)	Standardized hydrogen production cost (yuan per kilogram)
Alkaline electrolyzer electrolyzing water to produce hydrogen—source of renewable energy on the way	Green hydrogen	80%	2.37
Alkaline electrolyzer electrolyzing water to produce hydrogen - Offshore renewable energy	Green hydrogen	76.34%	2.64
Hydrogen production by methane steam reforming - Carbon capture	Green hydrogen	68%	1.7
Gasification of food waste for hydrogen production	Blue hydrogen	78.34%	2.91
This article's process	Green hydrogen	83.3%	2.53

5. CONCLUSION

This paper proposes a multi-path collaborative hydrogen production system in high-altitude regions, fully utilizing the abundant local biomass and solar resources. The technical feasibility of water electrolysis hydrogen production and biomass–CO_2 electrolysis hydrogen production pathways is verified through chemical process simulation, and the economic feasibility is further validated through comparison with other technologies. The following conclusions are obtained:

(1) Proton exchange membrane (PEM) water electrolysis technology fully adapts to the intermittency of solar radiation in high-altitude regions, achieving hydrogen production entirely based on renewable energy. Biomass hydrogen production technology, by coupling with solar thermal technology to provide heat and steam gasification agents, enables the gasification process to be driven by renewable energy, realizing the synergistic utilization of biomass and solar energy.

(2) The biomass gasification process coupled with CO_2 electrolysis technology reduces carbon emissions while increasing hydrogen yield. The biomass gasification process makes full use of energy and achieves relatively high energy efficiencies, which are 36.1% and 35%, respectively.

(3) The hydrogen production yield and total gas yield of the system increase with the increase in temperature and decrease with the increase in input energy. The hydrogen production yield and total gas yield reach their maximum values when the wheat straw input energy is 430 kW and the reactor temperature is 800°C.

(4) Compared with other technologies, the collaborative hydrogen production pathway has higher capital and operational investments (approximately 20% higher), but it has advantages in terms of levelized cost of hydrogen. Meanwhile, the cost of the process proposed in this paper is relatively sensitive to renewable energy input.

REFERENCES

[1] Zhang Qiwei, Wei Yazhi, Chen Bin, et al. Current Status and Thoughts on the Development of Green Hydrogen Industry under the Dual-Carbon Goals [J]. Power Technology,2025,49(11):2269-2278.

[2] Zou Canying, Li Jianming, Zhang Xian, et al. Current Status, Technological Progress, Challenges and Prospects of the Hydrogen Energy Industry [J]. Natural Gas Industry,2022,42(04):1-20.）

[3] Wang Xin, Cui Ziyuan, Ma Xiaojuan, et al. Research Progress on Modeling and Optimization of Green Hydrogen Supply Chain [J]. Clean Coal Technology,2026,32(02):310-326.

[4] Wang Meng, Yu Dezhi, Fan Xiangyang, et al. Review on Green Hydrogen Production Methods and Innovative Technologies [J]. Power Supply Technology,2025,49(11):2259-2268.

[5] Yang Lanxiang. Performance Analysis and Evaluation of Coalbed Methane Hydrogen Production Coupled with Proton Exchange Membrane Fuel Cell System [D]. Hunan University of Technology,2024.

[6] Zhang Yu, Ma Changning, Wang Xiulin, et al. Research Progress on Hydrogen Production and Purification Technology from Natural Gas [J]. Modern Chemical Industry2025,45(03):61-65.

[7] Wang Liuying. Preparation of Modified Nickel-Based Catalysts and Research on Hydrogen Production from Xylene Steam Reforming Catalyzed by Them [D]. Nanjing University of Information Science and Technology,2025.

[8] Lu Jun, Guo Aoxue, Wang Kunjie, et al. Integrated Research on Wind-Solar-Thermal Coupled Electrolysis Water Splitting for Hydrogen Production [J/OL]. Chinese Journal of Chemical Engineering 1-15[2026-03-30]. https://link.cnki.net/urlid/11.1946.TQ.20251121.1056.006.

[9] Zhao Jiahao, Chen Yijiang, Sun Yihan, et al. Research Progress on Integrated Photothermal Hydrogen Production Catalytic Materials [J/OL]. Materials Report,1-24[2026-03-30].https://link.cnki.net/urlid/50.1078.tb.20260321.1054.004

[10] Li Chunyan, Wu Chenghuang, Xie Kaigui, et al. Water-Energy-Carbon Synergistic Optimization of an Integrated Energy System for Hydrogen Production from Desalinated Water [J]. Power System Technology,2026,50(02):564-575.

[11] Wang Jing, Li Peng, Li Zhen, et al. Development and Prospect of Biohydrogen Production Technology for Carbon Neutrality [J/OL]. Journal of Harbin Institute of Technology,1-19[2026-03-30].https://link.cnki.net/urlid/23.1235.T.20260321.1219.002.

[12] Tian Yu, Xu Yixun, Xu Yongle, et al. Optimal Operation of Park Integrated Energy System Considering Electro-hydro Coupling and Double-layer Uncertainties [J] Power automation equipment,2025,45(10):177-185.

[13] Chen Youxin, Zhang Kuan, Liu Nian, et al. Time Series Production Simulation Method for Electric-Hydrogen-Ammonia-Thermal Multi-energy Coupled Rural Distributed Energy System [J/OL] Power System Automation, 1-14[2026-03-30]. https://link.cnki.net/urlid/32.1180.TP.20260302.1016.004.

[14] Huang Liuyan, Wu Zhihua, Zhang Chenxi, et al. Modeling and Simulation of Alkaline Electrolysis Water Hydrogen Production System [J]. Thermal Power Generation,2026,55(03):110-118.

[15] Ma Yunan, Wang Peng, Qian Jin, et al. Research Progress and Prospects of High Current Density Proton Exchange Membrane Water Electrolysis for Hydrogen Production [J/OL]. Energy Research and Management, 1-9[2026-03-30]. https://link.cnki.net/urlid/36.1310.TK.20260303.0850.002.

[16] Wang Haiyun, Xiao Guiyou, Ba桑robu, et al. Thoughts on Promoting the Transformation and Development of Clean Energy in Xizang through New Quality Productivity [J]. Northwest Hydropower,2025,(05):137-141.

[17] Zheng Hongwei. Innovation of the Development Model for New Energy Projects in Xizang Based on Full Life Cycle Management - Taking Photovoltaic Power Generation as an Example [J]. China Strategic Emerging Industries,2025,(29):99-101.

[18] Bai Xiaoxia, Zhang Xiangyu, Jia Rongrong, et al. Research on the Construction and Application Path of the Green Hydrogen and Green Oxygen System in Xizang Based on "Electricity - Hydrogen - Oxygen" Multi-energy Coupling [J]. Guangdong Chemical Industry,2025,52(23):82-84+89.

[19] Wright M P. SOME EFFECTS OF HIGH ALTITUDE ON MAN[J]. The Lancet, 1956, 268(6955): 1263.

[20] Horri B A, Ozcan H. Green hydrogen production by water electrolysis: Current status and challenges[J]. Current opinion in green and sustainable chemistry, 2024, 47: 100932.

[21] Khalilnejad A, Sundararajan A, Sarwat A I. Performance evaluation of optimal photovoltaic-electrolyzer system with the purpose of maximum hydrogen storage[C]//2016 IEEE/IAS 52nd Industrial and Commercial Power Systems Technical Conference (I&CPS). IEEE, 2016: 1-9.

[22] Xue Qiangkun, Xu Hongpeng, Jia Ming, et al. Thermodynamic Study of a Hydrogen Production System from Wheat Straw Supercritical Water Gasification Coupled with Heat Storage [J]. Solar Energy Journal,2024,45(09):170-178.

[23] Wang Lu, Xu Zhilian, Jin Hao, et al. Hydrogen Production Technology of Photovoltaic Coupled Modular PEM Electrolyzer [J]. Petroleum and Natural Gas Chemistry,2025,54(03):79-85.

[24] Rodrigo R R, Martín R D, Fernández M B, et al. Technical and economic study of solar energy concentration technologies (linear Fresnel and parabolic trough collectors) to generate process heat at medium temperature for the dairy industry of Spain[J]. Solar Energy, 2024, 271: 112420.

[25] Yang Shiguan, Zhao Jiale, Zhang Chuanhao, et al. Simulation of Biomass Gasification for Hydrogen Production Based on Different Gasifiers [J]. Clean Coal Technology,2025,31(09):50-60.

[26] Oh, Sebin, et al. "Food waste gasification integrated with electrochemical reduction of carbon dioxide for advanced hydrogen production: Energy, techno-economic, and environmental analyses." Energy Conversion and Management 345 (2025): 120